ZnCdSe/ZnCdMgSe quantum well infrared photodetector

Arvind P. Ravikumar,[1,*] Adrian Alfaro-Martinez,[2] Guopeng Chen,[3] Kuaile Zhao,[3] Maria C. Tamargo,[2] Claire F. Gmachl,[1] and Aidong Shen[3]

[1]*Department of Electrical Engineering, Princeton University, Princeton, New Jersey 08544, USA*
[2]*Department of Chemistry, The City College of New York, New York 10031, USA*
[3]*Department of Electrical Engineering, The City College of New York, New York 10031, USA*
[*]*aravikum@princeton.edu*

Abstract: We report the design, fabrication and characterization of a II-VI $Zn_{0.51}Cd_{0.49}Se$ / $Zn_{0.45}Cd_{0.42}Mg_{0.13}Se$-based quantum well infrared photodetector (QWIP) with a bound to quasi-bound transition centered at 8.7 μm. The good growth quality of the epitaxial layers was verified by x-ray diffraction measurements. Absorption and photocurrent measurements yield results consistent with conventional III-V QWIPs. Photocurrent measurements reveal an exponential decrease with temperature. In addition, we also observe more than 4 orders of magnitude increase in photocurrent with applied bias. By compensating the drop in temperature performance with an increase in applied bias, we achieve an operating temperature of up to 140K and a responsivity of 1-10 μA/W.

OCIS codes: (040.5160) Photodetectors; (040.4200) Multiple quantum well.

References and links

1. S. D. Gunapala and S. V. Bandara, "Quantum Well Infrared Photodetector (QWIP) Focal Plane Arrays," in *Intersubband Transitions in Quantum Wells: Physics and Device Applications I*, H.C. Liu, and F. Capasso, eds. (Academic Press, 2000), pp. 197–282.
2. S. Krishna, D. Forman, S. Annamalai, P. Dowd, P. Varangis, T. Tumolillo, Jr., A. Gray, J. Zilko, K. Sun, M. Liu, J. Campbell, and D. Carothers, "Demonstration of a 320x256 two-color focal plane array using InAs/InGaAs quantum dots in well detectors," Appl. Phys. Lett. **86**(19), 193501 (2005).
3. S. Tsao, H. Lim, W. Zhang, and M. Razeghi, "High operating temperature 320x256 middle-wavelength infrared focal plane array imaging based on an InAs/InGaAs/InAlAs/InP quantum dot infrared photodetector," Appl. Phys. Lett. **90**(20), 201109 (2007).
4. H. Lu, A. Shen, M. C. Tamargo, W. Charles, I. Yokomizo, M. Munoz, Y. Gong, G. F. Neumark, K. J. Franz, C. Gmachl, C. Y. Song, and H. C. Liu, "Study of intersubband transitions of $Zn_xCd_{1-x}Se/Zn_{x'}Cd_{y'}Mg_{1-x'-y'}Se$ multiple quantum wells grown by molecular beam epitaxy for midinfrared device applications," J. Vac. Sci. Technol. B **25**, 1103–1107 (2007).
5. W. O. Charles, A. Shen, K. Franz, C. Gmachl, Q. Zhang, Y. Gong, G. F. Neumark, and M. C. Tamargo, "Growth and characterization of $Zn_xCd_{1-x}Se/Zn_{x'}Cd_{y'}Mg_{1-x'-y'}Se$ asymmetric coupled quantum well structures for quantum cascade laser applications," J. Vac. Sci. Technol. B **26**, 1171–1173 (2008).
6. H. Lu, A. Shen, M. C. Tamargo, C. Y. Song, H. C. Liu, S. K. Zhang, R. R. Alfano, and M. Munoz, "Midinfrared intersubband absorption in $Zn_xCd_{1-x}Se/Zn_{x'}Cd_{y'}Mg_{1-x'-y'}Se$ multiple quantum well structures," Appl. Phys. Lett. **89**, 131903 (2006).
7. B. S. Li, A. Shen, W. O. Charles, Q. Zhang, and M. C. Tamargo, "Multiple intersubband absorption in wide band gap II-VI $Zn_xCd_{1-x}Se$ multiple quantum wells with metastable zincblende MgSe barriers," Appl. Phys. Lett. **92**(26), 261104 (2008).
8. A. Shen, H. Lu, W. Charles, I. Yokomizo, M. C. Tamargo, K. J. Franz, C. Gmachl, S. K. Zhang, X. Zhou, R. R. Alfano, and H. C. Liu, "Intersubband absorption in $CdSe/Zn_xCd_yMg_{1-x-y}Se$ self-assembled quantum dot multilayers," Appl. Phys. Lett. **90**(7), 071910 (2007).
9. K. J. Franz, W. O. Charles, A. Shen, A. J. Hoffman, M. C. Tamargo, and C. Gmachl, "ZnCdSe/ZnCdMgSe quantum cascade electroluminescence," Appl. Phys. Lett. **92**(12), 121105 (2008).
10. Y. Yao, A. Alfaro-Martinez, K. J. Franz, W. O. Charles, A. Shen, M. C. Tamargo, and C. F. Gmachl, "Room temperature and narrow intersubband electroluminescence from ZnCdSe/ZnCdMgSe quantum cascade laser structures," Appl. Phys. Lett. **99**(4), 041113 (2011).

#172521 - $15.00 USD Received 12 Jul 2012; revised 10 Sep 2012; accepted 11 Sep 2012; published 17 Sep 2012

11. M. Sohel, X. Zhou, H. Lu, M. N. Perez-Paz, M. Tamargo, and M. Muñoz, "Optical characterization and evaluation of the conduction band offset for ZnCdSe/ZnMgSe quantum wells grown on InP(001) by molecular-beam epitaxy," J. Vac. Sci. Technol. B **23**(3), 1209–1211 (2005).
12. O. Zakharov, A. Rubio, X. Blase, M. L. Cohen, and S. G. Louie, "Quasiparticle band structures of six II-VI compounds: ZnS, ZnSe, ZnTe, CdS, CdSe, and CdTe," Phys. Rev. B Condens. Matter **50**(15), 10780–10787 (1994).
13. C. Sirtori, F. Capasso, J. Faist, and S. Scandolo, "Nonparabolicity and a sum rule associated with bound-to-bound and bound-to-continuum intersubband transitions in quantum wells," Phys. Rev. B Condens. Matter **50**(12), 8663–8674 (1994).
14. H. C. Liu, Z. R. Wasilewski, M. Buchanan, and H. Chu, "Segregation of Si δ doping in GaAs-AlGaAs quantum wells and the cause of the asymmetry in the current-voltage characteristics of intersubband infrared detectors," Appl. Phys. Lett. **63**(6), 761–763 (1993).
15. E. C. Larkins, H. Schneider, S. Ehret, J. Fleißner, B. Dischler, P. Koidl, and J. D. Ralston, "Influences of MBE growth processes on photovoltaic 3-5 μm intersubband photodetectors," IEEE Trans. Electron. Dev. **41**(4), 511–518 (1994).
16. Z. R. Wasilewski, H. C. Liu, and M. Buchanan, "Studies of Si segregation in GaAs using current-voltage characteristics of quantum well infrared photodetectors," J. Vac. Sci. Technol. B **12**(2), 1273–1276 (1994).
17. E. Kim, A. Madhukar, Z. Ye, and J. C. Campbell, "High detectivity InAs quantum dot infrared photodetectors," Appl. Phys. Lett. **84**(17), 3277–3279 (2004).
18. Z. Ye, J. C. Campbell, Z. Chen, E. Kim, and A. Madhukar, "InAs quantum dot infrared photodetectors with $In_{0.15}Ga_{0.85}As$ strain-relief cap layers," J. Appl. Phys. **92**(12), 7462–7468 (2002).
19. M. Ershov, H. C. Liu, M. Buchanan, Z. R. Wasilewski, and V. Ryzhii, "Photoconductivity nonlinearity at high excitation power in quantum well infrared photodetectors," Appl. Phys. Lett. **70**(4), 414–416 (1997).

1. Introduction

Quantum Well Infrared Photodetectors (QWIPs) have been extensively studied over the past decades chiefly for their application in thermal imaging as large area focal plane arrays [1–3]. The faster response time and compatibility with standard fabrication methods makes these detectors a promising alternative to the widely used HgCdTe and InSb based detectors in the mid-infrared (mid-IR) regime.

Aside from the traditional III-V material systems, the II-VI ZnCdSe / ZnCdMgSe system grown lattice matched to InP is being investigated as a potential material for developing intersubband (ISB) devices [4–10]. Combined with the dual advantage of a large conduction band offset (~1.12 eV [11]) and the absence of intervalley scattering [12], the ZnCdSe/ZnCdMgSe system is best suited for short-wavelength ISB devices. However, compared to III-V materials, the II-VI compounds have a higher electron effective mass. While this reduces the strength of the optical dipole matrix element, it allows designs with thinner barrier layers to prevent tunneling. In effect, II-VI materials can accommodate more active stages than III-V materials for the same total thickness of the structure. Previous studies on this system have already demonstrated ISB absorption in multiple-quantum well (MQW) designs [6–8]. There have also been recent reports on electroluminescence from ZnCdSe/ZnCdMgSe based Quantum Cascade emitter structures [9, 10]. Despite continued efforts in this direction, there have so far been no reports on QWIPs based on this material system. In this paper, we report the demonstration of a QWIP based on a ZnCdSe/ZnCdMgSe quantum well structure.

2. QWIP design and fabrication

The QWIP was designed based on a bound-to-quasibound transition with a theoretical absorption maximum at 10.0 μm. The quantum well sates were computed within a one-band conduction band model approximation with an energy dependent effective mass that accounts for band mixing [13]. The epi-layers consist of 50 periods of 41Å $Zn_{0.51}Cd_{0.49}Se$ wells doped to $5x10^{18}$ cm^{-3} separated by 150Å $Zn_{0.45}Cd_{0.42}Mg_{0.13}Se$ barriers, grown lattice matched to a semi-insulating InP substrate by Molecular Beam Epitaxy (MBE). They were sandwiched between thick, highly doped ZnCdSe (Cl: $5x10^{18}$ cm^{-3}) top and bottom contacts with thickness 4000Å and 8000Å, respectively. Prior to the growth of the II-VI epi-layers, a 1500Å InGaAs layer was deposited to prepare a uniform surface for subsequent II-VI growth.

#172521 - $15.00 USD Received 12 Jul 2012; revised 10 Sep 2012; accepted 11 Sep 2012; published 17 Sep 2012

Figure 1 shows the high-resolution X-ray diffraction pattern of the grown wafer taken using a Bruker D8 Discover XRD – clear satellite peaks indicate good growth quality. The period of the MQW is calculated using the formula, $d = \frac{\lambda}{2\cos(\theta)\Delta\theta}$, where λ is the wavelength of the x-ray (1.54056Å for Cu K_{α}^{1} line), θ is the Bragg angle of the substrate, and Δθ is the angular spacing between adjacent satellite peaks. The measured thickness of one period of the epi-layer was 201Å, corresponding to a 5% deviation from the design. The wafer was processed into 310 μm x 485 μm rectangular mesas by conventional lithography and wet- chemical etching. Finally, Ti/Au (250Å/3000Å) was evaporated for top and bottom contacts. The top contact has a window (300 μm x 300 μm) to allow for light absorption in Brewster angle geometry (Fig. 1 inset).

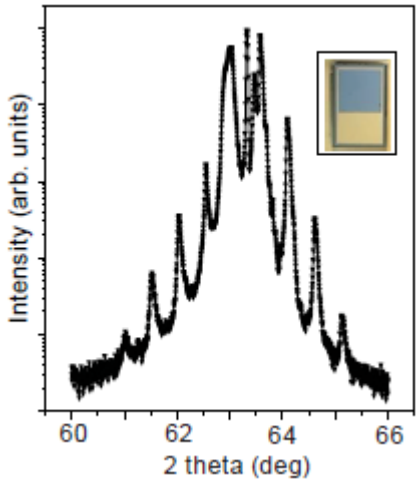

Fig. 1. X-ray diffraction (XRD) data measured from the QWIP structure prior to processing. The clearly differentiated satellite peaks indicate good structural quality of the sample. The thickness of a single period of ZnCdSe/ZnCdMgSe was computed to be 201Å, corresponding to a 5% deviation from the design period of 191 Å. (Inset) Optical image (top-view) of the QWIP used in the measurements: the device dimensions are 310 x 485 μm., while the window measures 300 x 300 μm.

3. QWIP characterization

Figure 2 shows the intersubband absorption and photocurrent spectra as measured using a Fourier Transform Infrared Spectrometer (FTIR). The absorption measurements were carried out in a 45 degree multi-pass transmission geometry at room temperature. The absorption peak at 8.7 μm with a full width at half maximum (FWHM) of 307 cm^{-1} ($\Delta\lambda/\lambda$ = 27%) deviates from the designed peak at 10 μm because of the deviation of the structural parameters (well thickness, alloy composition, etc.) from the designed values and a lack of accurate material parameters for some of the II-VI compounds. The photocurrent spectrum was taken at 78K with an applied bias of −2 V in Brewster's angle geometry, with the incident beam chopped at 150 Hz to facilitate detection using lock-in techniques. The peak wavelength in the photocurrent spectrum at 8.2 μm with a FWHM of 237 cm^{-1} ($\Delta\lambda/\lambda$ = 20%) is blue-shifted from the absorption peak at 8.7 μm mainly due to the difference in temperature (78K vs. 300K) and applied bias (0V vs. −2V).

#172521 - $15.00 USD Received 12 Jul 2012; revised 10 Sep 2012; accepted 11 Sep 2012; published 17 Sep 2012

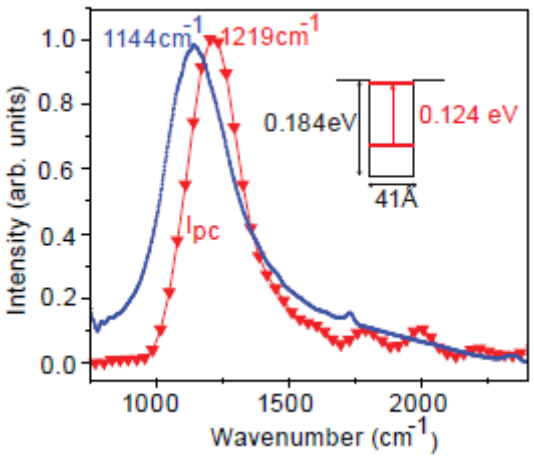

Fig. 2. Normalized absorbance of an unbiased wafer at room temperature (blue line) and photocurrent spectrum (red triangles) of a –2 V biased QWIP at 78 K. The shift in wavelength is attributed to the different temperature and bias employed in the photocurrent measurements. (Inset) A schematic of the quantum well design with the associated transitions and energy levels.

The performance of a QWIP is chiefly limited by the dark current. Figure 3(a) shows the plot of dark current as a function of temperature from 80 K to 300 K. Dopant segregation in the quantum wells may be the likely origin of the asymmetry in the current-voltage (IV) curves [14–16]. The dark current increases exponentially with temperature [17, 18] as revealed from a logarithmic plot of current as a function of inverse temperature shown in Fig. 3(b), at different operating voltages. The dark current noise power spectral density, being proportional to the dark current, degrades the signal to noise ratio and consequently the detectivity as dark current increases. The activation energy (near 0 V), E_{act}, defined as the energy difference between the Fermi level and the top of the barrier is given by $I = I_0 \exp(^{-E_{act}}/_{k_B T})$, where I is the dark current, I_o is a fit parameter and k_B is the Boltzmann constant. Fitting the dark current curves and extrapolating to 0 V gives a value for the activation energy of about 80 meV, in reasonable agreement with the calculated value of 88 meV. In the limit of low applied bias, E_{act} decreases linearly with increasing bias.

#172521 - $15.00 USD Received 12 Jul 2012; revised 10 Sep 2012; accepted 11 Sep 2012; published 17 Sep 2012

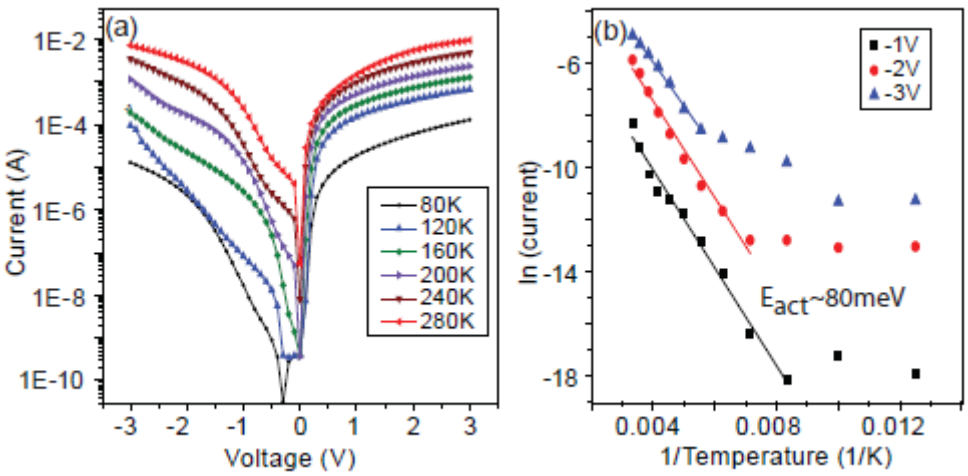

Fig. 3. (a) Dark current characteristics of the QWIP as a function of temperature from 80 K to 280 K. (b) Logarithmic plot of the dark current as a function of inverse temperature, at different applied bias. The slope of the plot gives an estimate of the activation energy, which in the case of –3V (blue triangles), –2V (red circles) and –1V (black squares) is 72 meV, 80.5 meV and 81 meV, respectively.

We also measure the photocurrent using a Daylight Solutions Inc. continuous wave Quantum Cascade laser tunable between 1000 cm^{-1} and 1120 cm^{-1}, slightly off the peak absorption wavenumber of 1144 cm^{-1}. Similar to the photocurrent measurement, shifting the spectral measurement to 150 Hz greatly improves the signal-to-noise ratio by eliminating the DC dark current component. Figure 4(a) shows the photocurrent data at 78K as a function of applied bias. As can be seen, the photocurrent increases by about 3 orders of magnitude even at a small applied bias of 0.5 V, which follows from the photoconductive nature of the QWIP – any small change away from the flat-band condition would induce a significant increase in the escape probability of an electron from the quantum well and therefore the photocurrent. In addition, the photocurrent also reduces exponentially with temperature, as seen from Fig. 4(b), which shows a logarithmic plot of photocurrent taken at 1085 cm^{-1} as a function of inverse temperature. It is important to note that this exponential degradation is due to the exponential increase in dark current with temperature, manifested in the measurement as the difference in voltage across the device between dark and illuminated conditions. Temperatures beyond 120K and voltage below 2V resulted in a photocurrent below the dark-current noise-level of the measurement. However, the photocurrent increases by more than 4 orders of magnitude upon applying a bias, as shown in Fig. 4(c) taken at 80K and 1085 cm^{-1}. Combining these two opposing effects, it is possible to achieve high temperature operation by appropriately compensating degrading temperature performance with an applied bias, as shown in Fig. 4(d). With this technique, we were able to measure photocurrent response up to 140K, despite the large dark current values (see Fig. 3(a)). The peak responsivity of the detector at the operating conditions of 80K and 1.5 V applied bias is about 1-10 μA/W, with the low values being chiefly attributed to the large dark current.

#172521 - $15.00 USD Received 12 Jul 2012; revised 10 Sep 2012; accepted 11 Sep 2012; published 17 Sep 2012

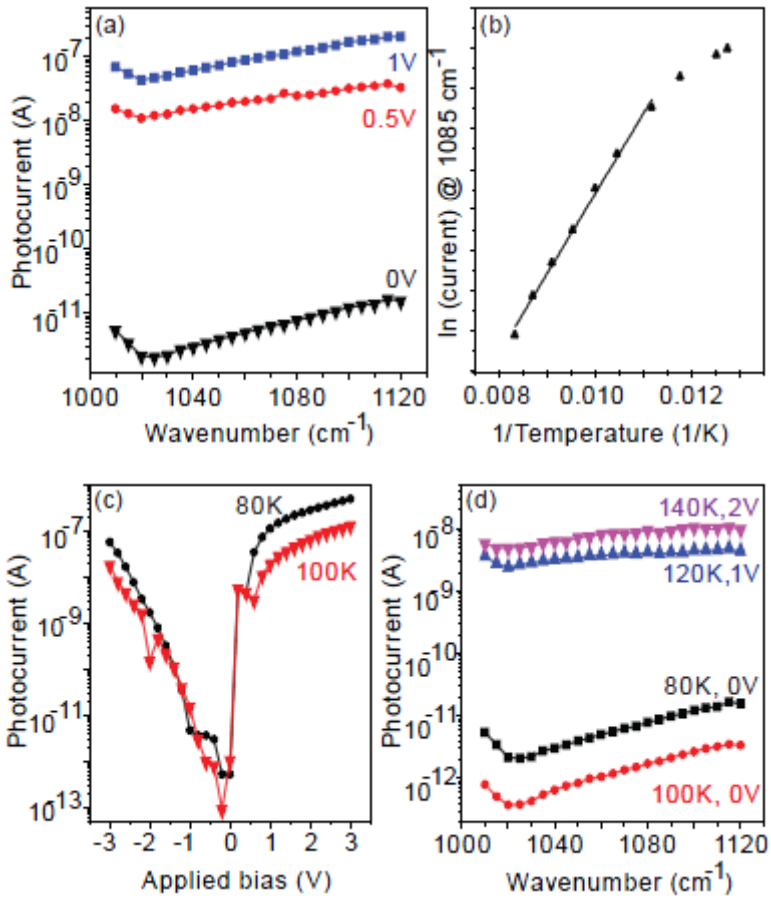

Fig. 4. (a) Narrowband photocurrent spectra taken at 78K near the peak absorption wavelength using a tunable Daylight Solutions Inc. laser as a function of applied bias. Note the four orders of magnitude change in photocurrent with bias. (b) Logarithmic plot of photocurrent at 1085 cm^{-1} indicating an exponential decay with temperature. (c) Responsivity measured at 78K and 1085 cm^{-1} as a function of applied bias – notice the asymmetric behavior as seen in the dark current curves in Fig. 2 at low temperature. In addition, we also observe a four orders of magnitude change in photocurrent and responsivity between 0 and –3 V applied bias. (d) Photocurrent spectra at temperatures between 80K and 140K, taken by compensating degrading temperature performance with applied bias.

Figure 5(a) shows the response of the detector measured at 1085cm^{-1} as a function of incident light power at 78K. It is non-linear indicating a saturation of the photocurrent for powers exceeding 160 mW. This is likely due to nonlinear effects in the QWIP at low applied bias, resulting in the formation of multiple electric field domains [19]. A more detailed analysis of this effect is beyond the scope of this paper. We believe that this dynamic range can be improved with a lower doping concentration in the active region.

#172521 - $15.00 USD Received 12 Jul 2012; revised 10 Sep 2012; accepted 11 Sep 2012; published 17 Sep 2012

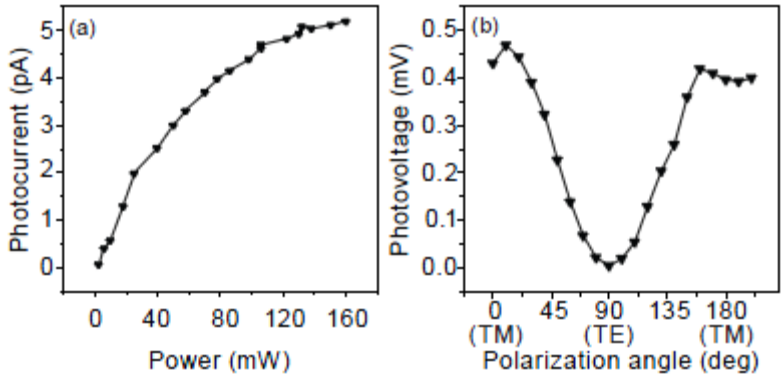

Fig. 5. (a) Photocurrent measurement, taken at 1085cm^{-1} near the peak absorption wavelength, as a function of laser power, indicating saturation at higher power. (b) Photocurrent as a function of polarization angle, with a TM/TE rejection ratio of over 100, confirming intersubband absorption over thermal effects.

Intersubband excitation has been further confirmed with polarization dependent measurements by rotating the incident laser polarization. Figure 5(b) shows the measured photocurrent values at 78K and 1085cm^{-1}, as a function of polarization angle, showing a TM/TE rejection ratio of over 100. In addition, we have also tested the device for photocurrent response far away from the absorption peak using an in-house Quantum Cascade laser at 4 μm. The measured photocurrent was below the noise level of the lock-in amplifier.

3. Conclusion

In summary, we demonstrate the development of a QWIP based on the II-VI ZnCdSe/ZnCdMgSe material system. Intersubband absorption spectra measured using an FTIR showed a broad peak centered around 8.7 μm (FWHM 308 cm^{-1}), while the photocurrent spectrum was blue-shifted to 8.2 μm (FWHM: 237cm^{-1}). Photocurrent measurements using a Daylight Solutions Inc. laser indicated an exponential decay of the signal with increasing temperature. Coupled with the more than 4 orders of magnitude change in photocurrent with applied bias, we were able to achieve an operating temperature of 140 K by compensating degrading temperature performance with increasing applied bias. Further optimization of design and doping is beyond the scope of this work.

Acknowledgments

The authors would like to acknowledge Peter Qiang Liu for providing the 4 μm Quantum Cascade laser for measurements. This work is supported in part by MIRTHE (NSF-ERC # EEC-0540832), NSF grant # ECCS- 1028364 and NSF grant # HRD-0833180.

#172521 - $15.00 USD Received 12 Jul 2012; revised 10 Sep 2012; accepted 11 Sep 2012; published 17 Sep 2012